PERFORMANCE OF MEMS-BASED GAS DISTRIBUTION AND CONTROL SYSTEMS FOR SEMICONDUCTOR PROCESSING

Albert K. Henning, John Fitch, James M. Harris, Errol B. Arkilic, Brad Cozad, and Edward B. Dehan
Redwood Microsystems, Inc.
959 Hamilton Avenue, Menlo Park, CA 94025

Biography

Albert K. Henning received the A.B. and A.M. degrees from Dartmouth College in Physics in 1977 and 1979, respectively. From 1979 to 1982 he was a device physicist with Intel in Santa Clara, CA. From 1982 to 1987 he was a research assistant at Stanford University, receiving the Ph.D. (E.E.) in 1987. From 1987 to 1995, he was Assistant and Associate Professor of Engineering Science at Dartmouth College. He spent portions of the 1993-94 academic year on sabbatical, as a Visiting Scientist in the Microstructures Technology Laboratory at MIT. In 1996 he joined Redwood Microsystems, as Program Manager and as Wafer Fab Manager.

His interests in MOSFET device physics focused on the development of scanning probe microscopy for dopant profiling, technology characterization and failure analysis. He has worked with colleagues in physics, mechanical engineering, and biomedical engineering in the research and development of novel, microscale devices, including SiGe transistors, thermocouple MOSFETs, and a variety of mechanical and fluidic MEMS devices. He received an Analog Devices Career Development Professorship in 1987, and an IBM Faculty Development Award in 1990. He
has published over fifty journal and proceedings articles, has received one U.S. patent, and has several patent applications in process. He is a member of Sigma Xi, ASEE, and IEEE.

Abstract

The advent of MEMS (micro-electro-mechanical systems) has enabled dramatic changes in diverse technological areas. In terms of control and distribution of liquids and gases (microfluidics), MEMS-based devices offer opportunities to achieve increased performance, and higher levels of functional integration, at lower cost, with decreased size and increased reliability. Microfluidic actuators include distribution microchannels and orifices, microvalves, micropumps, and microcompressors. Related microsensors are required to measure temperature, flow, pressure, viscosity, and density.

This work focuses on recent research and product development of high-purity gas distribution and control systems for semiconductor processing. These systems include the following components, based upon both normally-open and normally-closed microvalves: pressure-based mass flow controllers (PMFCs) [1]; vacuum leak-rate shut-off valves; and pressure regulators. Advanced packaging techniques enable these components to be integrated into gas sticks and panels which have small size, corrosion-resistant wetted materials, small dead volumes, and minimal particle generation. Principles of operation of components and panels, and performance data at both the component and system level, will be presented. The potential for 10x size reduction (linear dimension), 2x product yield improvement (through increased reliability, improved flow accuracy and repeatability, and contamination reduction), and 5x reduction in process gas and liquid consumption, will also be addressed.

Introduction

Previous MEMS work has demonstrated the performance of: thermopneumatically-actuated microvalves [2]; other micro-fabricated valves [3]; pressure and flow regulation using such valves [4]; microflow control using electrostatic valves [5]; and integrated, pressure-based mass-flow control [6]. Most mass-flow controllers (MFCs) today are thermal MFCs (TMFCs). They do not use MEMS-based components, but instead rely on the time-of-flight of a thermal pulse launched into a portion of the gas stream [7]. This work demonstrates the high accuracy and repeatability available using pressure-based, as compared to thermal, mass-flow control. It demonstrates the integration of several micro-fabricated components, which (with an appropriate flow model) facilitates the realization of a PMFC having: high resolution; a wide range of flow control capability; relatively low power consumption; well-controlled materials in the wetted path; and adequate response time. It discusses the derivation of pressure regulators from PMFCs. It presents a vacuum leak-rate shut-off valve, for use in MEMS-based fluid control and distribution systems. Finally, it discusses the integration of PMFCs, pressure-regulators, and vacuum leak-rate shut-off valves into a compact panel system for the control and distribution of gases and liquids used in semiconductor processing.

PMFC Flow Theory

The PMFC relies on analytical expressions for the flow through the fluidic elements of the device. These expressions are presented here.

As with TMFCs, the flow through the PMFC must be determined from sensor measurements. In this instance, however, the pressure upstream and downstream of a flow element (whether valve or orifice) is related to a calibrated flow model, in order to measure the flow. For gas flow, if there is no viscous loss, then the compressible flow model in the subsonic regime can be expressed as in Equation (1) [8]. δ is a parameter related solely to the ratio γ of specific heats (at constant pressure and volume) for the particular gas under control. R is the universal gas constant divided by the molecular weight of the gas. C_d is the coefficient of gas discharge for the flow element. P is the pressure either into, or out of, the flow element. T is the fluid temperature.

$$\dot{m} = \frac{P_{in}}{\sqrt{RT}} C_d A \left(\frac{P_{out}}{P_{in}}\right)^{1/\gamma} \delta(\gamma) \sqrt{\left(\frac{P_{in}}{P_{out}}\right)^{\frac{\gamma-1}{\gamma}} - 1} \quad (1)$$

Sonic flow is given in Equation (2). α is a parameter similar to δ. Flow in the microvalve itself rarely enters the sonic regime. However, the flow area of the valve must be determined either using a loss coefficient model [8], or some other means to relate the structural parameters (inlet area, and membrane-to-inlet gap) to the effective area. The valve and orifice have different values of C_d, between 0.7 and 0.9.

$$\dot{m} = P_{in} C_d A \frac{\alpha(\gamma)}{\sqrt{RT}} \quad (2)$$

Liquid flow for the PMFC is given in Equation (3). C_l is the coefficient of liquid discharge for the flow element. β is the flow element inlet-to-plumbing diameter ratio.

$$\dot{m} = C_l A \sqrt{\frac{2\rho(P_{in} - P_{out})}{1 - \beta^4}} \quad (3)$$

PMFC Principle of Operation

The PMFC is represented schematically in Figure 1. A ceramic package provides a modular foundation for the thermopneumatically-actuated microvalve, a flow orifice, two pressure sensors, and a temperature sensor. Specifications for the PMFCs are shown in Table I.

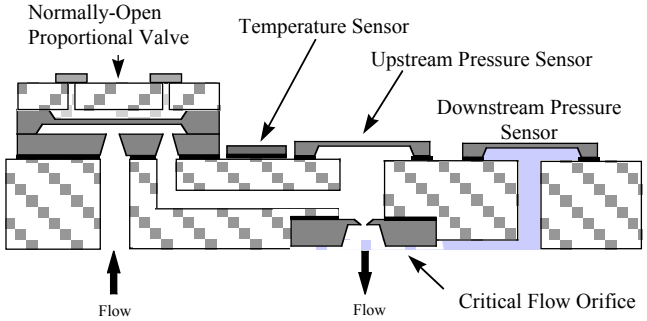

Figure 1: *Schematic representation of the PMFC.*

Fluid Media:	Gases/Liquids
Maximum Flow Rates:	1, 10, 100, 1000 sccm/ccm
Turndown Ratio:	5:1 (sonic); > 20:1 (subsonic)
Accuracy:	± 1% of F.S.
Repeatability:	± 0.1% of reading
Resolution:	± 0.1% of reading
Response Time:	500 ms typical
Inlet Pressure Range:	20 to 50 psig
Maximum Outlet Pressure:	200 Torr
Temperature Range:	0 to 50°C
Power Consumption:	1.5 W typical
Dimensions:	106 mm x 32 mm x 25 mm

***Table I**: Specification for PMFC.*

Figure 2 diagrams the system behavior, including feedback. In the following discussion, 'CO' refers to the flow orifice, and stands for 'critical orifice', even though the flow is not critical for liquids, and is occasionally sub-sonic for gases. 'NO' refers to the normally-open microvalve. The flow area of the CO is a constant. The effective flow area of the NO is proportional to the NO membrane stroke, which itself is governed by the power supplied to the microvalve. For gas flow through the CO in the sonic regime, the mass flow is linearly proportional to the absolute pressure upstream of the CO, as shown in Equation (2). The CO thus sets the flow range, consistent with the PMFC specification. Since the CO and NO devices are in series, the intersection of the flow models for each element determines both the sensed pressure P_x, and the mass flow. This principle is shown in Figure 3, where the PMFC module inlet pressure is 50 psia, and the module outlet pressure is 200 T. As the NO changes from 100 percent flow to lesser values of flow, the intersection of the NO and CO flow curves falls (the value of P_x falls), and the PMFC flow decreases.

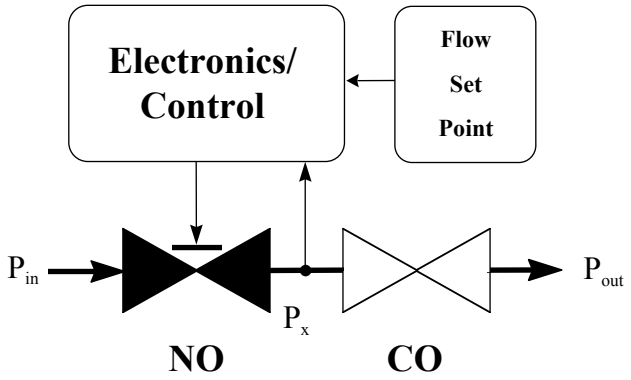

***Figure 2:** Schematic representation of the compressible flow model for the series combination of a normally-open proportional valve, and a critical orifice.*

The CO also sets the flow resolution, as shown in Figure 4 for sonic flow. Taking the derivative of Equation (2) with respect to pressure upstream of the orifice creates the relationship between flow resolution and pressure resolution shown in this figure. For a given pressure sensor resolution and CO area, the minimum flow resolution becomes known. Thus, the CO determines not only the PMFC flow range, but also the minimum flow resolution.

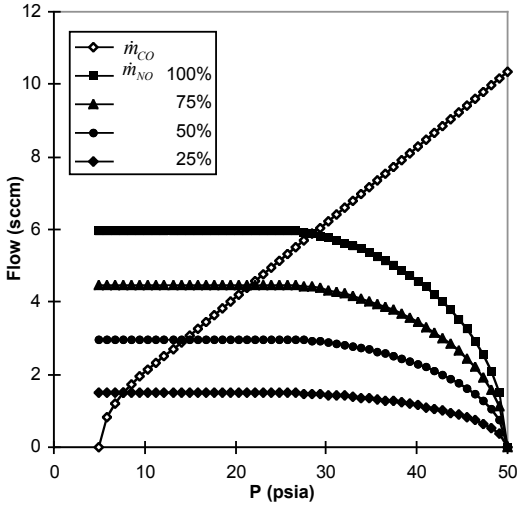

***Figure 3:** Flow model for a 5 sccm gas PMFC.*

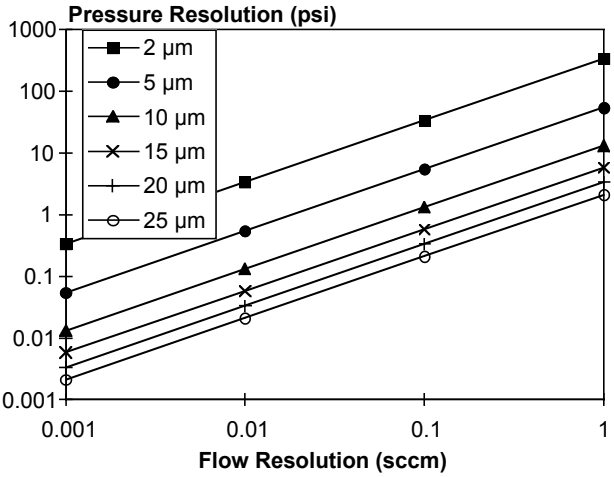

***Figure 4:** Pressure resolution required to achieve a given flow resolution, versus CO hydraulic diameter.*

PMFC Packaging and System Integration

Figure 5 shows the packaging associated with the PMFC. An on-board E^2PROM stores the flow calibration information which relates measured

pressure to derived flow, using the appropriate flow equations shown earlier. The ceramic module is attached to a stainless steel manifold, for inclusion of the PMFC into the overall fluid control and distribution system. The feedback control electronics, and their incorporation into this package, are also depicted.

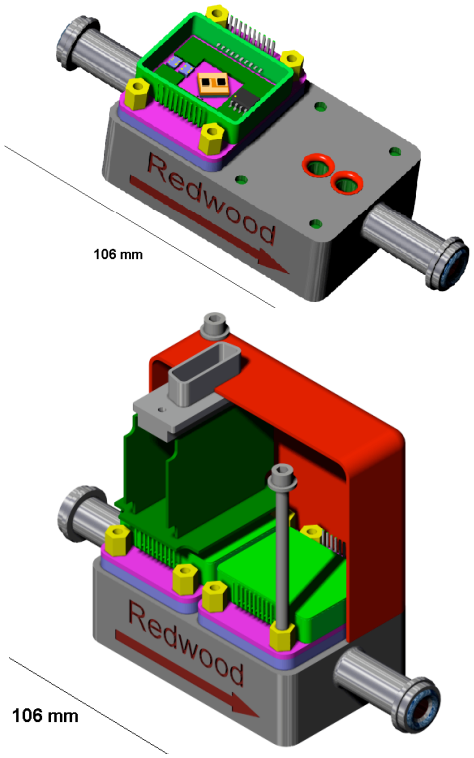

Figure 5: *(Top) A MEMS-based PMFC, showing a single module (with protective lid removed), mounted to a stainless steel manifold. The normally-open microvalve, two pressure sensors, and the E^2PROM containing the calibration coefficients, are visible. (Bottom) A two-module device, with a cut away enclosure revealing supporting electronics boards.*

PMFC Measurements

Figures 6-10 show measurements performed on a 10 sccm PMFC, as well as comparable TMFCs. The tests were performed under the SEMATECH specifications SEMASPEC #92071221 B-STD. The test system is based on a calibrated laminar flow element secondary standard, which is itself calibrated to a high-precision, rate-of-rise primary standard [9]. The figures demonstrate the PMFC has superior performance characteristics when juxtaposed with comparable TMFCs. It also has adequate response time for semiconductor process equipment applications.

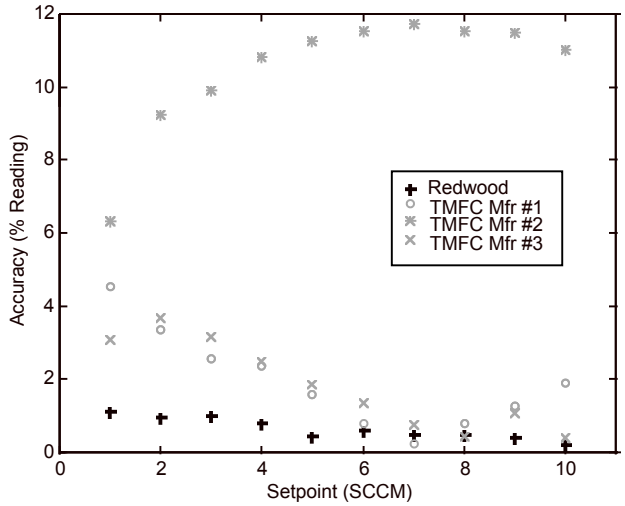

Figure 6: *MFC accuracy comparisons for PMFC (this work) and TMFCs (other units).*

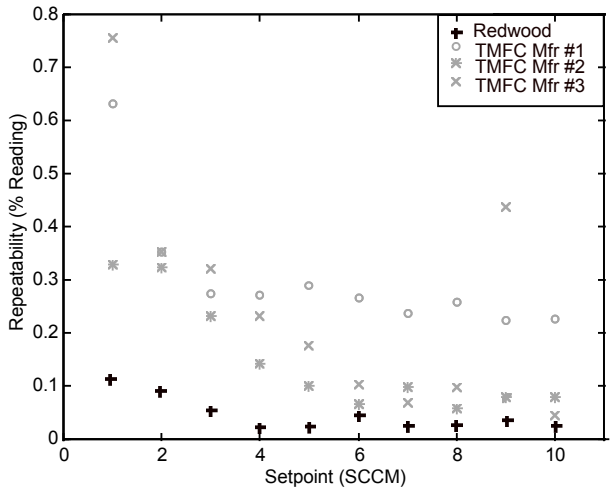

Figure 7: *MFC repeatability comparisons for PMFC (this work) and TMFCs (other units).*

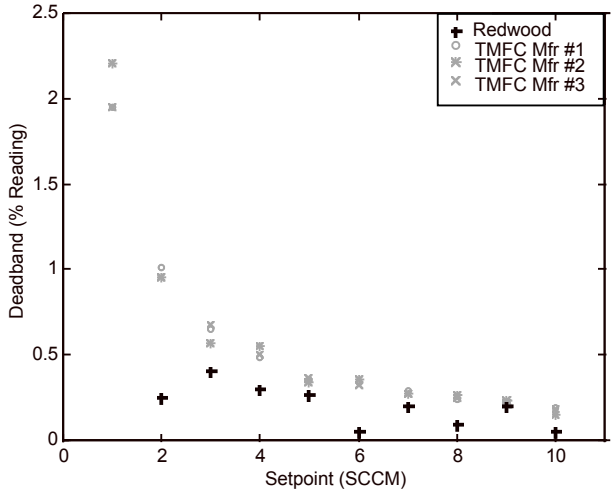

Figure 8: *MFC deadband (resolution) comparisons for PMFC (this work) and TMFCs (other units).*

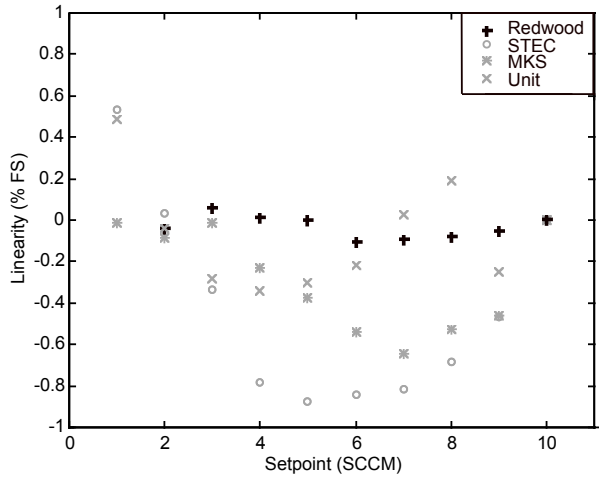

Figure 9: *MFC linearity comparisons for PMFC (this work) and TMFCs (other units).*

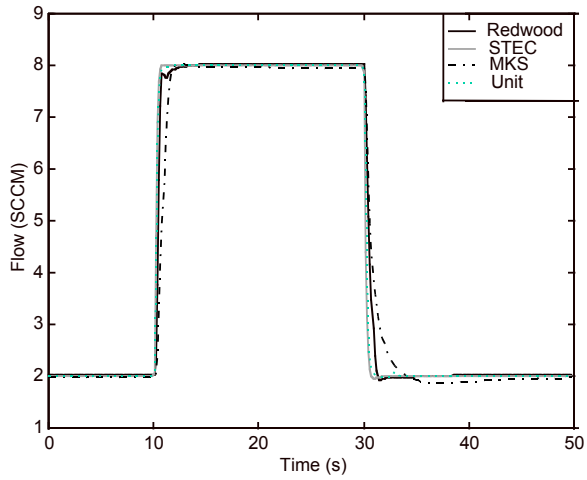

Figure 10: *MFC response time comparisons for PMFC (this work) and TMFCs (other units).*

PMFC Discussion

The MEMS-based PMFC offers several benefits relative to the TMFC. *Small size:* For 'plug and play' applications, the PMFC with steel manifold is roughly one inch by 2 inches by 3 inches high, including electronics. In module form only, the size decreases by more than a factor of two. If remote electronics are utilized, the vertical dimension shrinks to one-half inch. *Higher resolution:* The use of 16 bit A/D for the pressure sensor, and 16 bit D/A for the valve driver, enables very high resolution, which exceeds the SEMATECH specifications. *Materials compatibility:* The wetted path in the PMFC is comprised of silicon, alumina (ceramic), and appropriate die attach materials. As such, it facilitates flow of all semiconductor processing fluids, save those which contain ionic fluorine, or other ionic elements which etch silicon. *Lowered defect generation:* MFC-generated particles are understood to derive from the number of sealing surfaces, the internal surface roughness, and the internal volume. Compared to TMFCs, the number of seals is reduced, and the internal dead volume is decreased by a factor of two to four.

Some liquids of interest in semiconductor processing must be maintained at a relatively low temperature to assure stability. A thermopneumatically actuated microvalve may require temperatures which, at the heater resistor, exceed this threshold temperature. However, proper valve design ensures the silicon membrane contact surface will remain well below this threshold temperature [10].

Pressure Regulators

Pressure regulators are created from a subset of the components of the PMFC. Only a microvalve, temperature sensor, and a single pressure sensor are required (see Figure 1). No flow model is required to connect the pressure measured downstream of the valve to the overall flow. Control is effected by measuring the pressure, and throttling the microvalve's fluidic resistance until the difference between the setpoint pressure and the measured pressure is less than the specified error for the regulator.

Vacuum Leak-Rate Shut-Off Valves

Normally-closed (NC) valves are important components of other MEMS-based microvalve devices [11]. We have created NC valve modules which have a wetted path composed entirely of ceramic (Al_2O_3) or silicon. These valves also have incorporated a proprietary sealing technology, which enables very low leak rates to be obtained [12]. As with the NO valve (MFC or pressure regulator) modules, wetted surfaces may be coated with SiC or Si_3N_4, in order to provide materials compatibility in situations where a wetted silicon surface would be undesirable.

Figure 11 shows a cross-section of this normally-closed, low-leakage shut-off valve. The thermopneumatic actuation principle is still employed. In this case, however, a boss is added to the silicon membrane, and a silicon cantilever is either fusion-bonded to the boss. Under conditions of zero input power, this cantilever will provide the shut-off property by sealing against a low-leakage seat (polished silicon). As shown, the wetted path is entirely silicon or ESG-compatible ceramic. The silicon-ceramic interface is a eutectic bond. The overall dimensions are 8 mm x 6 mm x 2 mm, and are (roughly) to scale.

Figure 12 shows the schematic cross-section of the sealing interface between an elastomer (o-ring) and the polished silicon valve seat. The sealing force compresses the elastomer, as depicted. Approximately, the leak rate through the elastomer, as a function of pressure drop, gas diffusion coefficient for the elastomer, and o-ring geometry, is:

$$\dot{m}_{leak} \equiv 2\pi R \cdot \Delta P \cdot k \cdot 2 \int_0^{y_{max}} \frac{dy}{2\sqrt{r^2 - y^2}} \qquad (4)$$

Our calculations based on Equation (4) encouraged the design and fabrication of the vacuum leak-rate NC valves. Figure 13 shows measured helium leak rates for a set of such devices. The sealing surfaces are comprised of two parts. The mechanically fixed surface is silicon. The movable cantilever's sealing surface contains either Viton®, Kel-F®, Chemraz®, or Kalrez®, in order to achieve the Sematech leak-rate specification of 1 x 10^{-9} atm-cc-He/sec. Also shown is data from a standard shut-off valve commonly used in the industry.

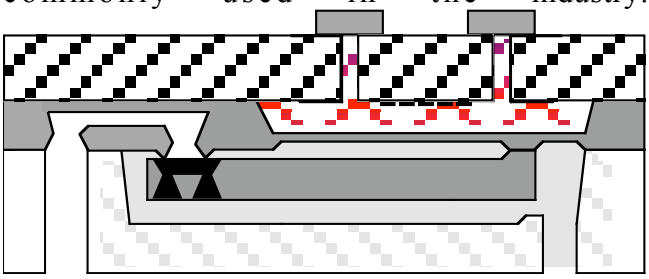

Figure 11: *Cross-section of a thermopneumatically-actuated, normally-closed, low-leakage shut-off valve.*

The SEMATECH specification for shut-off valves is less than 10^{-9} cc-He/sec after 15 seconds of shut-off. Shut-off valves used at present in the industry reach higher steady-state leak rates than these microvalves, due to their more permeable sealing materials, or smaller compression forces on the sealing surfaces. At the same time, the width of their sealing surfaces is greater than in our microvalve, occasionally resulting in lower metastable values of leak rate.

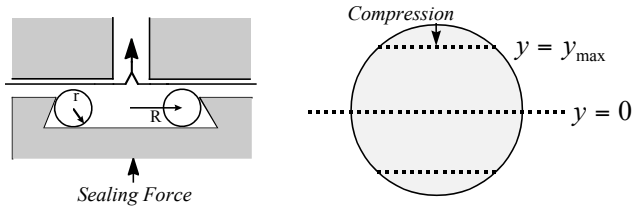

Figure 12: *Close-up schematic of sealing surfaces in MEMS-based vacuum leak-rate shut-off valve..*

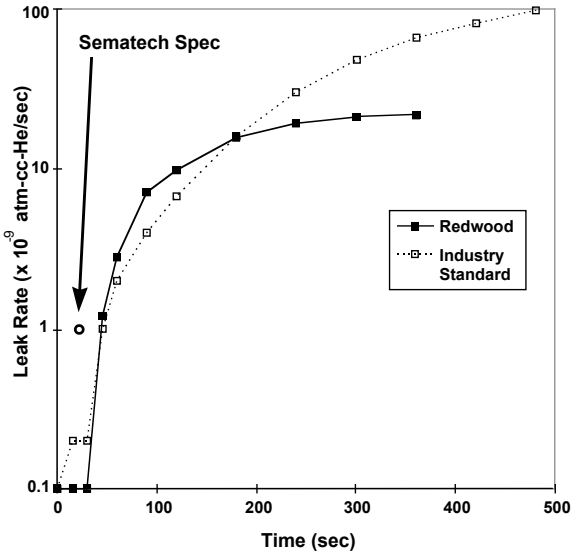

Figure 13: *Example of vacuum leak-rate data for MEMS-based shut-off valve..*

Overall System Integration

Figure 14 shows the natural extension of the modular concept of individual PMFCs, pressure regulators, and shut-off valves, into a complete, four-channel gas stick. Each channel consists of two vacuum leak-rate shut-off valves, a pressure regulator, and a PMFC. A purge line for the channels is also included. In Figure 14, it is assumed that the electronics control for the overall system is situated remotely, whereas for

an individual PMFC or pressure regulator, the electronics control is located directly above the MEMS module, as shown in Figure 5.

Figure 15 depicts the relative benefits of a MEMS-based gas distribution and control system, when compared with existing panels having identical functionality. The MEMS-based design occupies only six percent of the volume of 1995 panel designs, and only nine percent of the volume of 1996 designs. Welds are eliminate altogether, while the use of advanced seals (such as C-, W-, or Z-seals) remains constant, though they are themselves reduced in size.

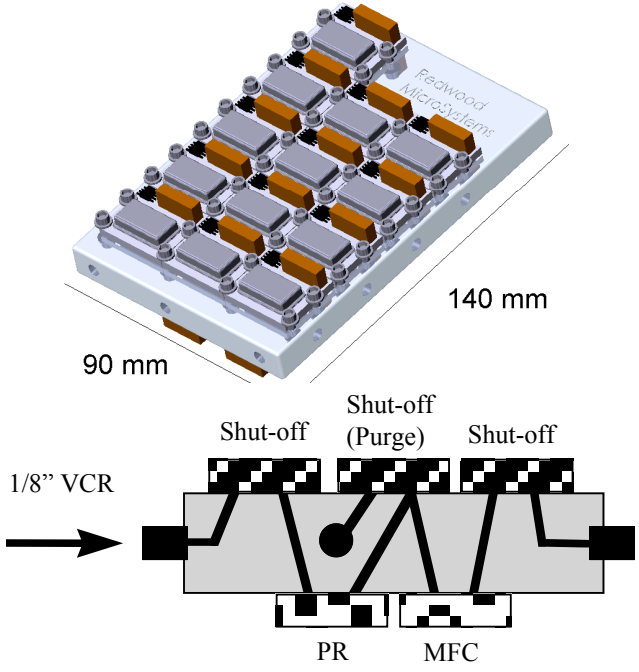

Figure 14: *(Top) Isometric view of a four-channel gas panel derived from PMFCs, as well as MEMS-based shut-off valves and pressure regulators; (Bottom) Schematic representation of the four-channel panel.*

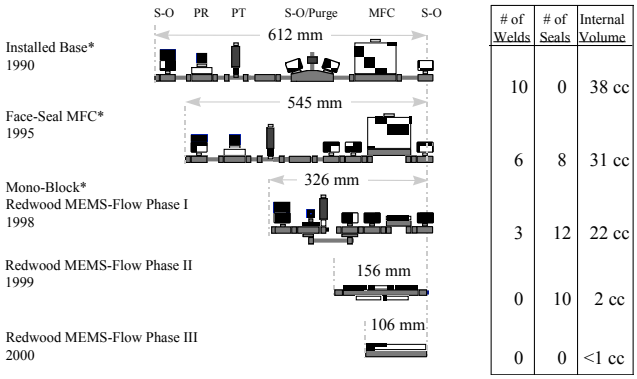

# of Welds	# of Seals	Internal Volume
10	0	38 cc
6	8	31 cc
3	12	22 cc
0	10	2 cc
0	0	<1 cc

Figure 15: *Size comparison of present and future integrated gas sticks/panels (after [13]).*

Conclusions

We have demonstrated the science and technology required to design and fabricate flow distribution and control devices suitable for the semiconductor processing industry. Components such as pressure-based flow models, calibrated flow orifices, pressure and temperature sensors, normally-open proportional valves, and normally-closed vacuum leak rate shut-off valves, have been developed. The valve actuation is based on prior thermopneumatic techniques. These components have been integrated into shut-off valve, mass flow controller, and pressure regulator modules, which themselves are combined at a higher level into integrated gas panels. Each integrated device has the benefit of small size, lower cost, higher resolution, materials compatibility, and lowered defect generation, which are among the most important attributes of the successful application of MEMS-based technology.

References

[1] A. K. Henning, "Microfluidic MEMS for semiconductor processing." In Proceedings, *Intl. Conf. on Innovative Systems in Silicon*, pp. 340-349 [IEEE Press, Piscataway, NJ, 1997].

[2] M. J. Zdeblick and J. B. Angell, In Proceedings, *Transducers '87 (1987 Int'l. Conf. Sol. State Sens. and Act.)*, pp. 827-829 [IEEE, Piscataway, NJ, 1987].

[3] P. W. Barth, "Silicon microvalves for gas flow control." In Proceedings, *Transducers '95 (1995 Int'l. Conf. Sol. State Sens. and Act.)*, pp. 276-279 [IEEE, Piscataway, NJ, 1995].

[4] M. Zdeblick, "Integrated, microminiature electric-to-fluidic valve and pressure/flow regulator." U.S. Patent 4,821,997 (1989).

[5] J. Robertson, "An electrostatically-actuated integrated microflow controller." Ph.D. dissertation, U. Michigan, 1996.

[6] M. Esashi, S. Eoh, T. Matsuo, and S. Choi, "The fabrication of integrated mass flow controllers." In Proceedings, *Transducers '87,* pp. 830-833 [Inst. Elec. Eng. Japan, 1987].

[7] G. Chizinsky, "Recent advances in mass flow Control." *Solid State Technology*, p. 85 (September, 1994).
[8] Frank M. White, Fluid Mechanics. McGraw-Hill (New York, 1979).
[9] E. B. Arkilic, M. A. Schmidt, and K. S. Breuer, "A technique for high resolution mass flow measurements at atmospheric pressures." *Experiments in Fluids* (1997).
[10] A. K. Henning, J. S. Fitch, D. J. Hopkins, Jr., L. Lilly, R. Faeth, E. Falsken, and M. J. Zdeblick, "A thermopneumatically actuated microvalve for liquid expansion and proportional control." In Proceedings, *Transducers '97 (1997 Int'l. Conf. Sol. State Sens. and Act.)*, pp. 825-828 [IEEE, Piscataway, NJ, 1997].
[11] See the Fluistor™ product literature and specifications from Redwood Microsystems (e.g., http://www.redwoodmicro.com).
[12] Patent applications in process.
[13] J. Cestari, D. Laureta, and H. Itafuji, "The next step in process gas delivery: a fully integrated system." *Semiconductor International*, January 1997, pp. 79-87.

Acknowledgments:
The efforts of M. Barrera, L. Christel, Y. Fathi, D. Hopkins, D. King, B. Kozen, L. Lilly, W. McCulley, W. Weber, and M. Zdeblick have been crucial in the development of the devices described in this work. The efforts of R. Abad, E. Falsken, G. Helstrom, K. Hirano, Y. Hua, R. Leni, A. Moreno, and K. Sterritt are gratefully acknowledged. This work has also been supported in part by DARPA, under Contract #DAAL01-94-C-3401.